Supporting Information

Carbon supported uniform RuAgW nanoparticles with high activity and CO resistance toward alkaline hydrogen oxidation

Hao Yang[a,#], Chunxiao Chai[a,#], Mengting Chen[a], Yongpeng Li[a], Zhongyu Qiu[a], Tiantian Li[a], Jiahuan Li[a], Desheng Wang[a], Shuo Han[a], Mengyu Yang[a], Xiaoxia Gao[b], Rui Gao[a], Yang Lv[a], Yujiang Song[*a]

[a] State Key Laboratory of Fine Chemicals, School of Chemical Engineering, Dalian University of Technology, 2 Linggong Road, Dalian 116024, China.

[b] Instrumental Analysis Center, Dalian University of Technology, 2 Linggong Road, Dalian 116024, China.

[#] These authors contributed equally to this work.

*** Corresponding authors:**

Prof. Yujiang Song

E-mail: yjsong@dlut.edu.cn

Experimental section.

Chemicals. Ruthenium chloride ($RuCl_3$, Ru content ≥ 35.8-38.0 wt%) was purchased from Shenyang Nonferrous Metals Research Institute Co., Ltd. Sodium tungstate dihydrate ($Na_2WO_4 \cdot 2H_2O$, purity ≥ 99%) was obtained from Energy Chemical Reagent Co., Ltd. Silver nitrate ($AgNO_3$, purity ≥ 99%) was received from Tianjin Bodi Chemical Co., Ltd. Sodium borohydride ($NaBH_4$, purity ≥ 98.0%), potassium hydroxide (KOH, purity ≥ 85.0%) and sodium hydroxide (NaOH, purity ≥ 98.0%) were ordered from Sinopharm Chemical Reagent Co., Ltd. 20 wt% Pt/C was purchased from Shanghai Hesen Electric Co., Ltd. Nafion resin solution (5 wt%) was obtained from DuPont. Anion Exchange Membrane (AEM, 25 μm) purchased from Huizhou Yiwei Hydrogen Energy Co., Ltd. Gas diffusion layer (GDL) was purchased from Sunrise Power Co., Ltd. All of the above reagents and chemicals were used as received without further purification. Vulcan XC-72 (VXC-72) carbon black was acquired from Akzo Nobel and pretreated in nitric acid (3 M) at 80 ℃ for 1 h and then washed to pH neutral before use. The ultrapure water (18.2 MΩ cm at 25 °C) was produced from a Millipore water system (Synergy® UV) and used in all experiments.

Synthesis of Catalysts. In a typical synthesis, 40 mg of VXC-72 was dispersed in 10.0 mL of ultrapure water under 3 min of sonication, after which 17.5 mg of $RuCl_3$, 0.8 mg of $AgNO_3$ and 1.6 mg of Na_2WO_4 $2H_2O$ were added under 10 min of sonication. Next, 4.3 mL of freshly prepared $NaBH_4$ aqueous solution (10 mg mL^{-1}) was added dropwise under stirring at 20 °C for 2 h. After washing with deionized water until the pH of the filtrate became neutral, the resulting black powder was dried in an oven at 65 °C

overnight. Finally, the black powder was placed in a tube furnace and heated at 250 °C for 2 h in argon atmosphere with a ramping rate of 5 °C min^{-1} from room temperature. For comparison, RuAg/C, RuW/C and Ru/C were synthesized using the same method while only varying the precursors.

Characterizations.

Transmission electron microscopy (TEM) was carried out on a Tecnai G2 F30 Spirit (FEI) operated at 120 keV. High-resolution TEM (HRTEM) and energy dispersive X-ray spectroscopy (EDS) elemental mapping were recorded on a JEM-F200 (JEOL, 200 keV). Powder X-ray diffraction (XRD) was conducted on a SmartLab 9 kW (Rigaku) with a Cu Kα radiation source (45 kV, 200 mA) in a 2θ range from 10° to 90° at a scanning rate of 10° min^{-1}. Thermogravimetric analysis (TGA) curves were recorded on a TA-Q600 in a temperature range from room temperature to 800 °C at a heating rate of 10 ℃ min^{-1} in dry air. Metal element components of the samples were determined by inductively coupled plasma optical emission spectroscopy (ICP-OES, 7300DV, Perkin Elmer). X-ray photoelectron spectroscopy (XPS) was performed on a ESCALAB XIþ (thermo, U.K.) to analyze the surface chemical state of materials. Binding energy of C1s (C-C) at 284.8 eV was used to carry out the calibration.

Electrochemical measurements.

Electrochemical measurements were carried out in a three-electrode system on a CHI 760D electrochemical work station (Shanghai Chenhua Instrument Co., Ltd) at 25 ℃. A glassy carbon electrode (5.0 mm in diameter) coated with electrocatalysts thin layer was used as the working electrode. A Hg/HgO (1 M NaOH aqueous solution) electrode

was served as the reference electrode and a graphite rod was used as the counter electrode. 3 mg of electrocatalyst powder was dispersed in a mixture of ultrapure water (18.2 MΩ·cm), 5 wt% Nafion solution, and ethanol at a volume ratio of 1:0.01:9 under mild sonication to obtain a homogeneous ink of 1 mg mL^{-1}. Then, the ink was dropped on the glassy carbon electrode and dried at room temperature. All potentials in this work were referenced to reversible hydrogen electrode (RHE). The conversion equation from Hg/HgO to RHE is $E(RHE) = E(Hg/HgO) + 0.904\ V$.

Cyclic voltammetry (CV) curves were conducted in a N_2-saturated 0.1 M KOH aqueous solution from 0.05 to 1.0 V vs. RHE with a scan rate of 50 mV s^{-1}. Alkaline HOR polarization curves (also known as linear sweep voltammetry curves, LSV curves) were tested under H_2-saturated 0.1 M KOH aqueous solution at a scan rate of 10 mV s^{-1} and 1600 rpm in the potential range from -0.1 to 0.3 V vs. RHE. Electrochemical impedance spectra (EIS) were recorded at open circuit voltage in a frequency range from 100 kHz to -0.1 Hz with a voltage perturbance of 5 mV. The real part of the resistance was used to obtained iR-free potential ($E_{iR\text{-}free}$) using the equation ($E_{iR\text{-}free}=E\text{-}iR$).

CO stripping experiments were used to estimate the oxophilicity and electrochemical active surface area (ECSA) of samples.[1] CO was firstly bubbled in 0.1 M KOH aqueous solution for 10 min to reach a full monolayer of adsorbed CO on the metal surface at a potential of 0.1 V vs. RHE. Next, N_2 was bubbled for another 10 min to completely purge CO, while keeping the potential at 0.1 V vs. RHE. CO stripping was conducted by cycling from 0.05 to 1.0 V vs. RHE with a scan rate of 20 mV s^{-1}.

CO resistance was evaluated by using the chronoamperometry method, also known as the I-t test. The current was recorded in the presence of 1000 ppm CO over time, while maintaining the voltage at 0.1 V vs. RHE and the electrode rotation speed of 1600 rpm.

Accelerated durability test (ADT) was carried out through the following two steps. Firstly, CV curves were collected by potential cycling from 0.05 to 0.5 V vs. RHE for 1000 cycles at a scanning rate of 100 mV s^{-1}. After the CV scanning, LSV curves were recorded in the H_2-saturated 0.1 M KOH aqueous solution for analyzing the durability of the electrocatalysts.

Anion exchange membrane fuel cells (AEMFCs) testing.

Anodic electrocatalyst ink was prepared by mixing electrocatalyst powder with ultrapure water and isopropanol at a volume ratio of 1:9 and a certain amount of Alkymer®I-250 ionomer under mild sonication for 10 min. Similarly, cathodic electrocatalyst ink was obtained by dispersing 60 wt% Pt/C using the same method. Membrane electrode assembly (MEA) was fabricated by spraying the anodic and cathodic ink to each side of AEM (about 4 cm^2) to attain an anodic and cathodic electrocatalyst loading of 0.2 mg_{metal} cm^{-2} and 0.4 mg_{metal} cm^{-2}, respectively. Afterwards, the MEA was immersed in 1 moL L^{-1} NaOH aqueous solution for 24 h for ion exchange, followed by washing 3 times with deionized water, and then sandwiched between two sheets of gas diffusion layer (GDL) with a pressure of about 6.8 MPa for 2 min at 25 °C. The anion exchange membrane fuel cells (AEMFCs) was firstly conditioned under N_2 at 100% relative humidity (RH) until the cell temperature reached

80 °C. The anode was supplied with H_2 at 400 mL min^{-1}, and the cathode was supplied with O_2 at 400 mL min^{-1} at 100% RH.

Calculation method of alkaline HOR exchange current density and ECSA.

Diffusion current density (j_d) was calculated by the equation (1). Kinetic current density (j_k) was extracted from Koutecky-Levich equation (2)[2].

$$\eta = -\frac{RT}{2F}\ln\left(1-\frac{j_d}{j_1}\right)\#(1)$$

$$\frac{1}{j}=\frac{1}{j_k}+\frac{1}{j_d}\#\ (2)$$

where η is overpotential, j_1 is H_2 diffusion-limited current density, j is measured current density, and F is Faraday constant (96485 C mol^{-1}).

Mass specific exchange current ($j_{0,m}$) was obtained by Bulter-Volmer equation (3) and micropolarization Bulter-Volmer equation (4)[3].

$$j_k = j_{0,m}\left(exp\frac{\alpha F}{RT}\eta - exp\frac{(\alpha-1)F}{RT}\eta\right)\#(3)$$

$$j_k \approx j = j_{0,m}\frac{\eta F}{RT}\#(4)$$

where α is charge transfer coefficient in equation (3) (from -20 mV to +20 mV vs. RHE) and (4) (from -5 mV to +5 mV vs. RHE).

ECSA was calculated according to equation (5).

$$ECSA = \frac{Q_{CO}}{m \times C}\#(5)$$

where Q_{CO} is integrated charge of CO adsorbed onto the surface of electrocatalysts; m is metal mass loading; C is the amount of electricity per unit area adsorbed by CO on the surface of electrocatalysts, specifically, C is 420 μC cm^{-2}.

The area specific exchange current density ($j_{0,s}$) is obtained in the same way as $j_{0,m}$,

with the difference that the former j_k is the area specific exchange current density and the latter j_k is the mass specific exchange current density. $j_{0,m}$ is related to $j_{0,s}$ in the following way. The connection between $j_{0,m}$ and $j_{0,s}$ is as follows:

$$j_{0,s}(mA\ cm^{-2}) = j_{0,m}(A\ g^{-1})/(ECSA(m^2\ g^{-1}) \times 10) \#(6)$$

Calculation method of d-band center.

Binding energy of -2 - 10 eV and corresponding counts (i.e., intensities) were selected, and the Shirley background was subtracted from the measured spectra with the XPS peak fitting software (XPSPEAK41). Binding energy was used as the x-axis and the intensity after background subtraction as the y-axis. D-band center was calculated as follows:

$$x_0 = \frac{\sum_{i=1}^{n} x_i\, y_i}{\sum_{i=1}^{n} y_i} \#(7)$$

Where x_0 represents the d-band center, x_i represents the binding energy and y_i represents the intensity after background subtraction.

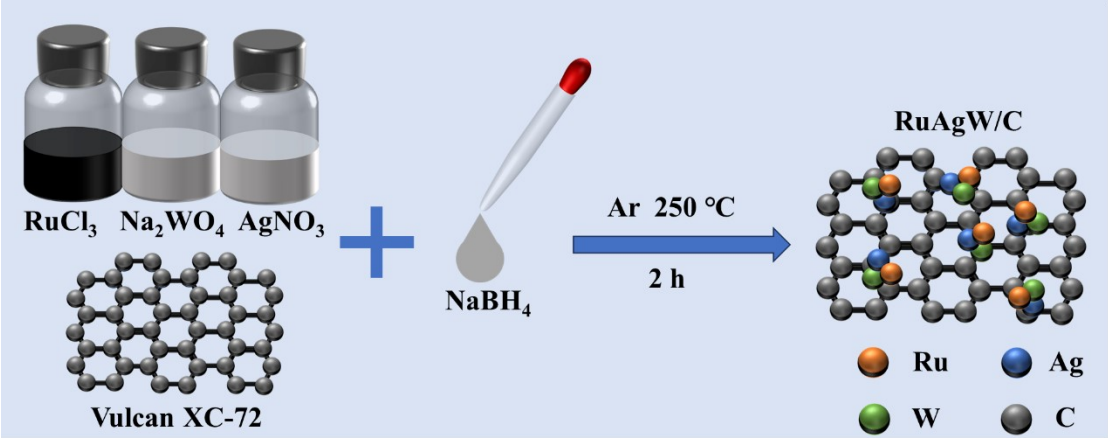

Figure S1. Synthetic scheme of RuAgW/C electrocatalyst.

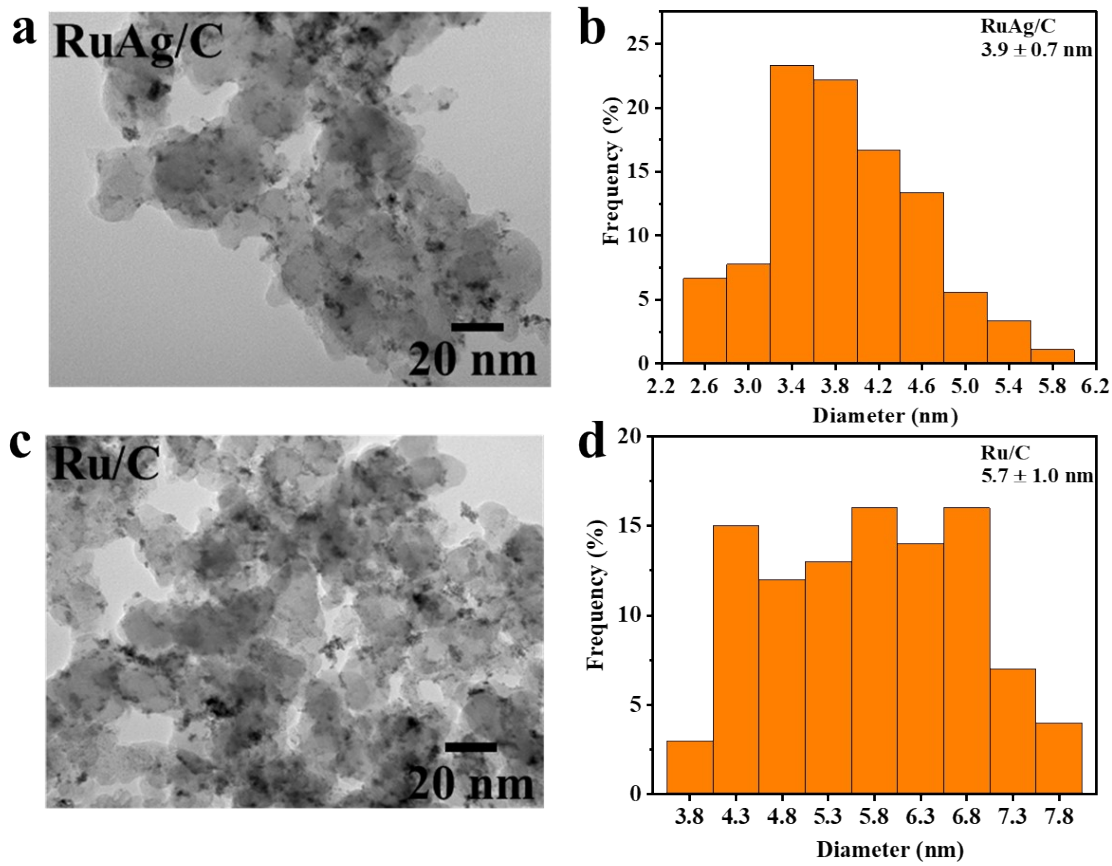

Figure S2. (a) A typical TEM image and (b) particle size distribution of RuAg/C; (c) a typical TEM image and (d) particle size distribution of homemade Ru/C. Note: the average size and size distribution for each sample were determined by manually measuring at least 200 individual particles.

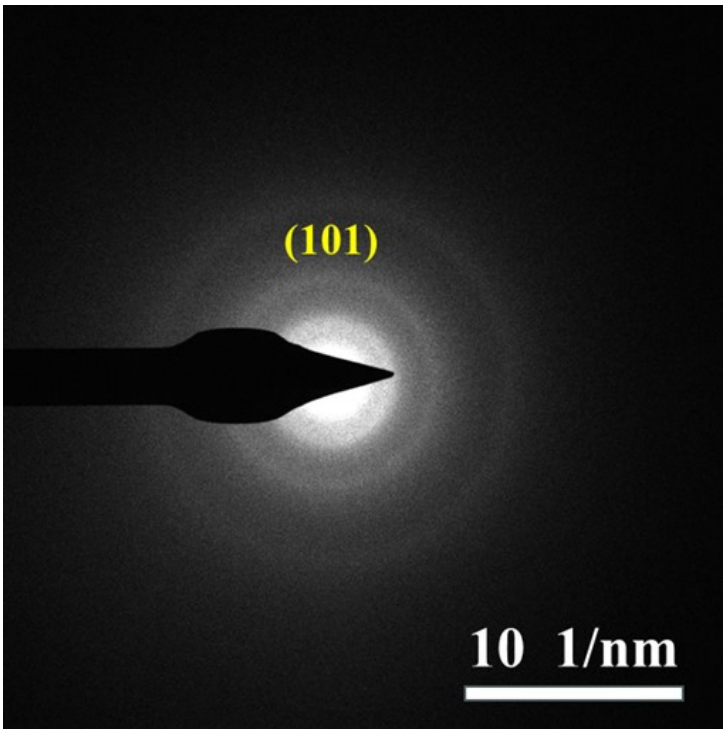

Figure S3. SAED pattern of RuAgW/C.

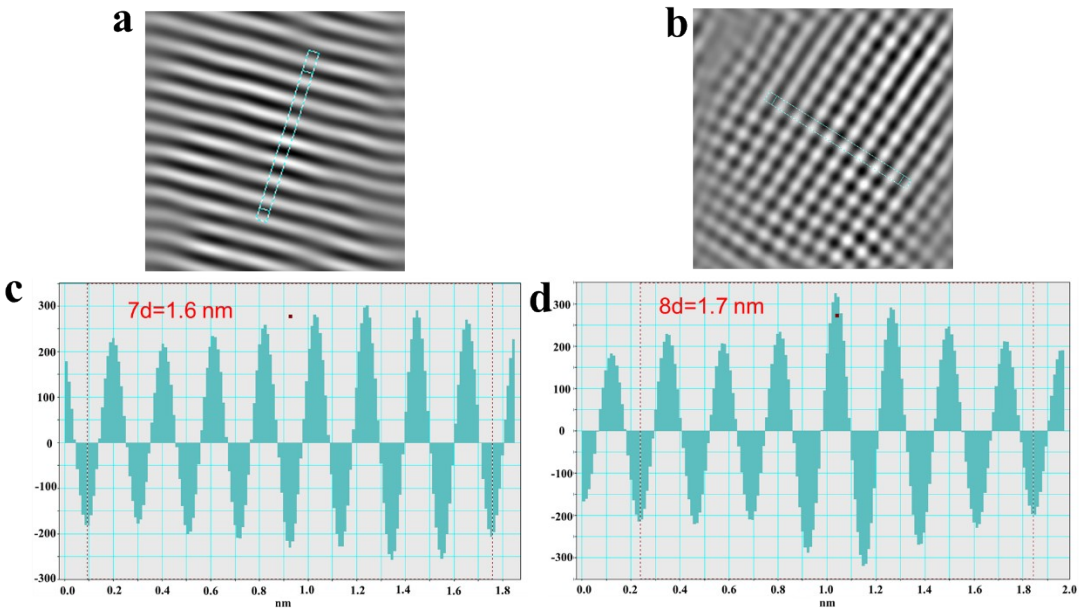

Figure S4. (a-b) FFT patterns and (c-d) corresponding lattice spacing of RuAgW/C along arrow indicated directions.

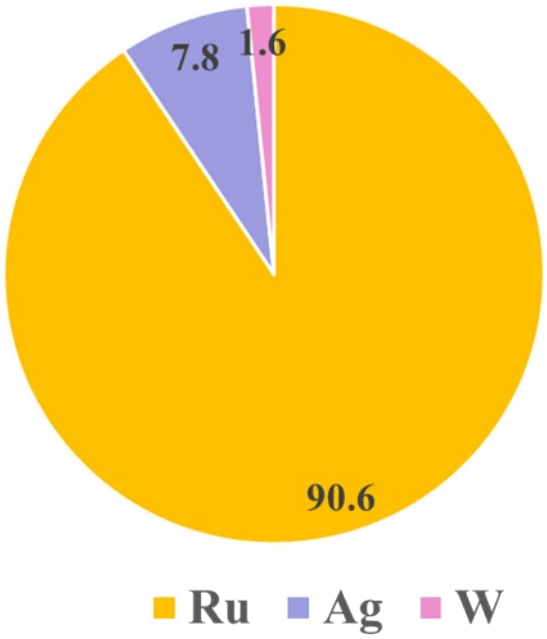

Figure S5. Molar ratio of Ru, Ag and W of RuAgW/C based on ICP-OES.

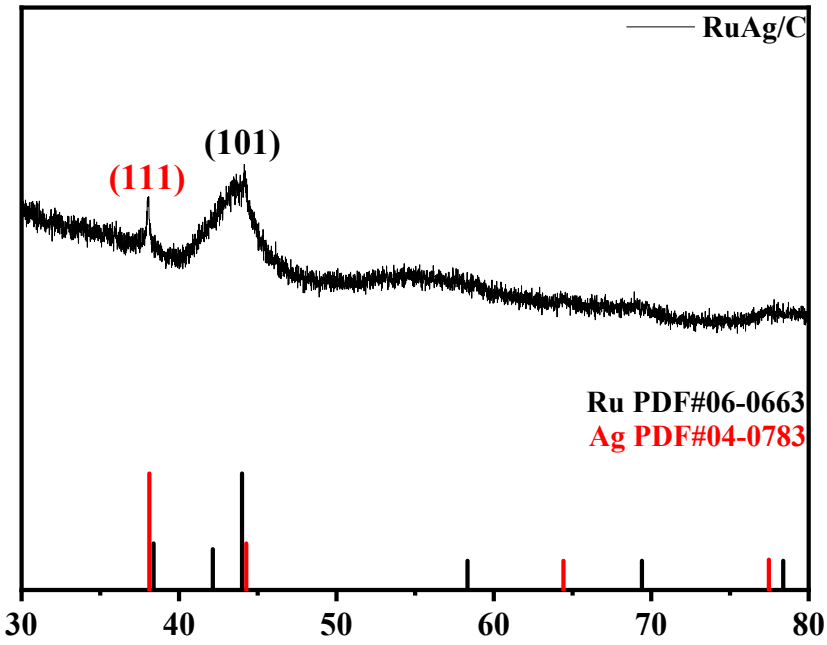

Figure S6. XRD pattern of RuAg/C.

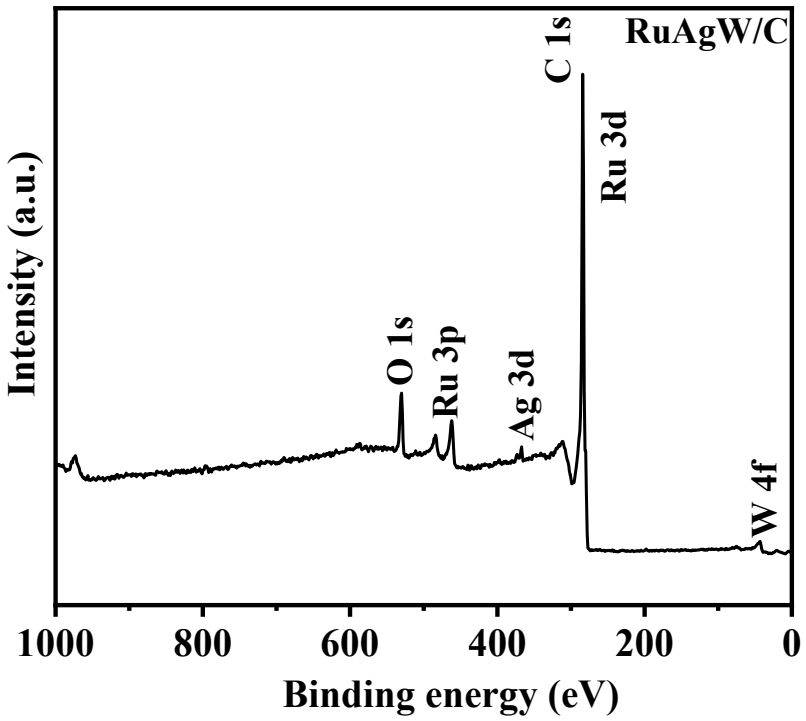

Figure S7. XPS full-spectrum of RuAgW/C.

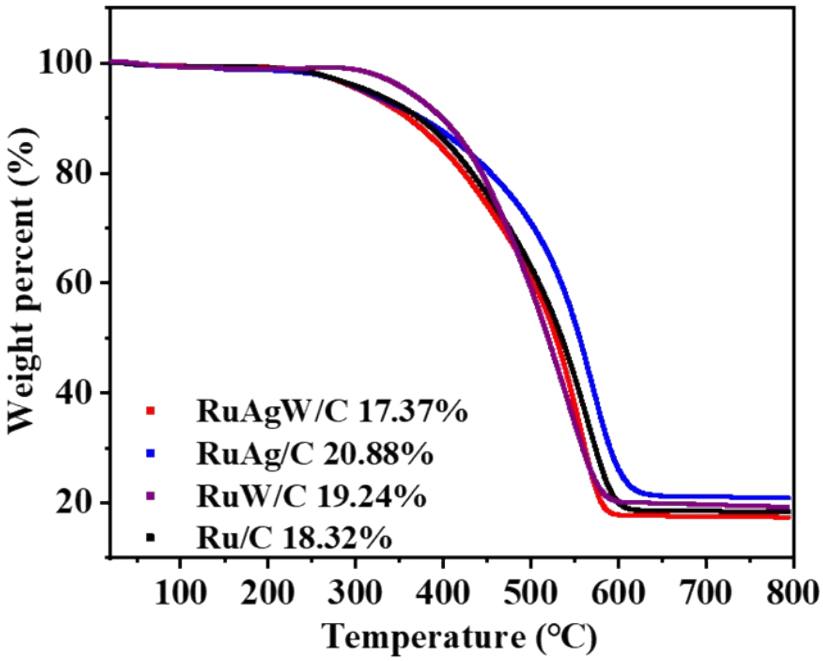

Figure S8. TGA curves of RuAgW/C, RuAg/C, RuW/C and homemade Ru/C.

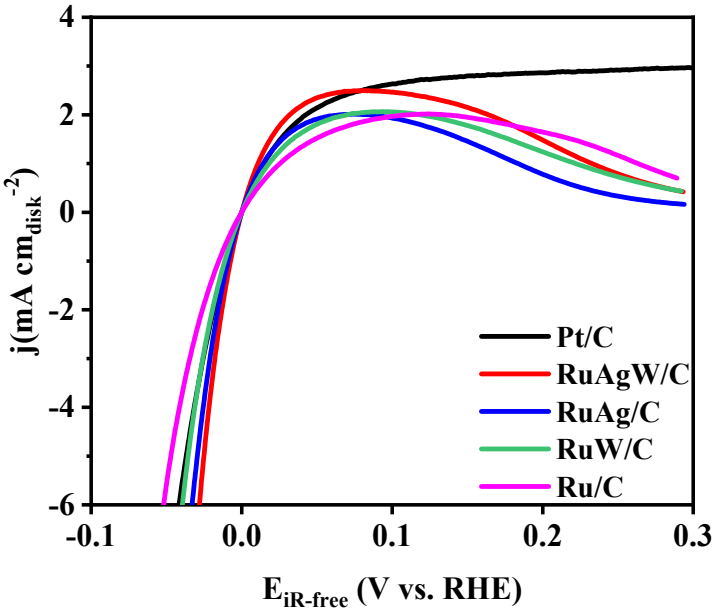

Figure S9. Alkaline HOR polarization curves of Pt/C, RuAgW/C, RuAg/C, RuW/C and homemade Ru/C.

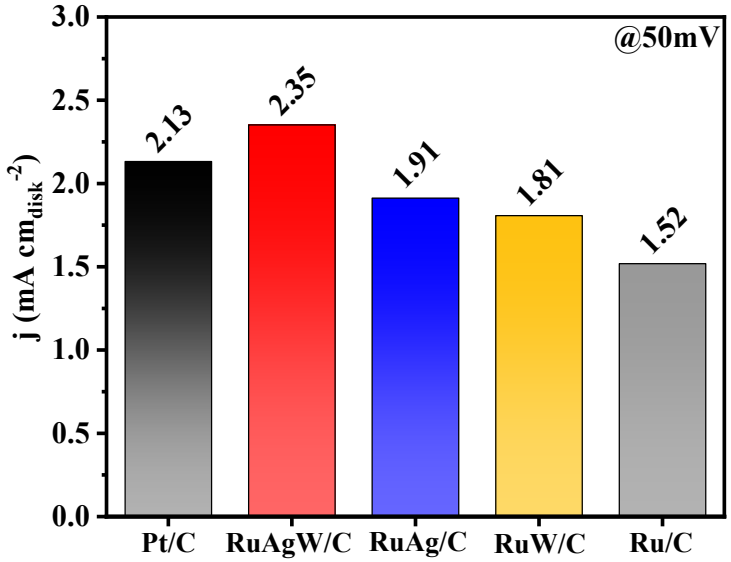

Figure S10. Current density at 50 mV vs. RHE of Pt/C, RuAgW/C, RuAg/C, RuW/C and homemade Ru/C.

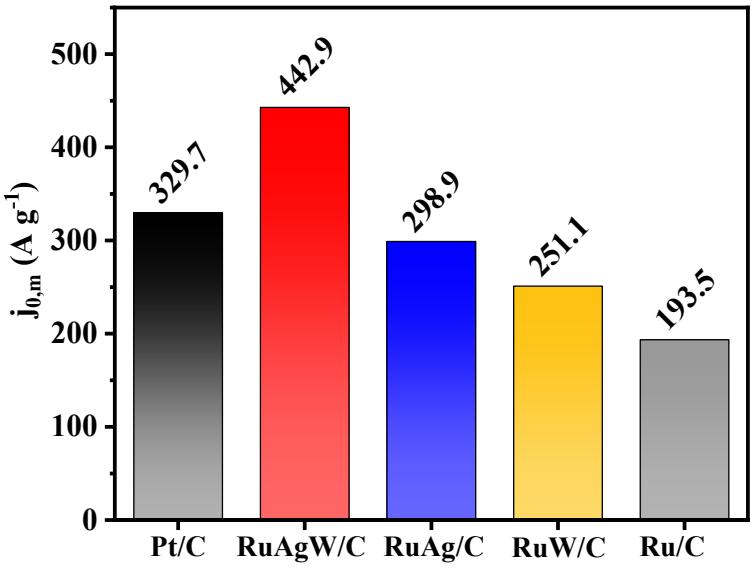

Figure S11. $j_{0,m}$ of Pt/C, RuAgW/C, RuAg/C, RuW/C and homemade Ru/C.

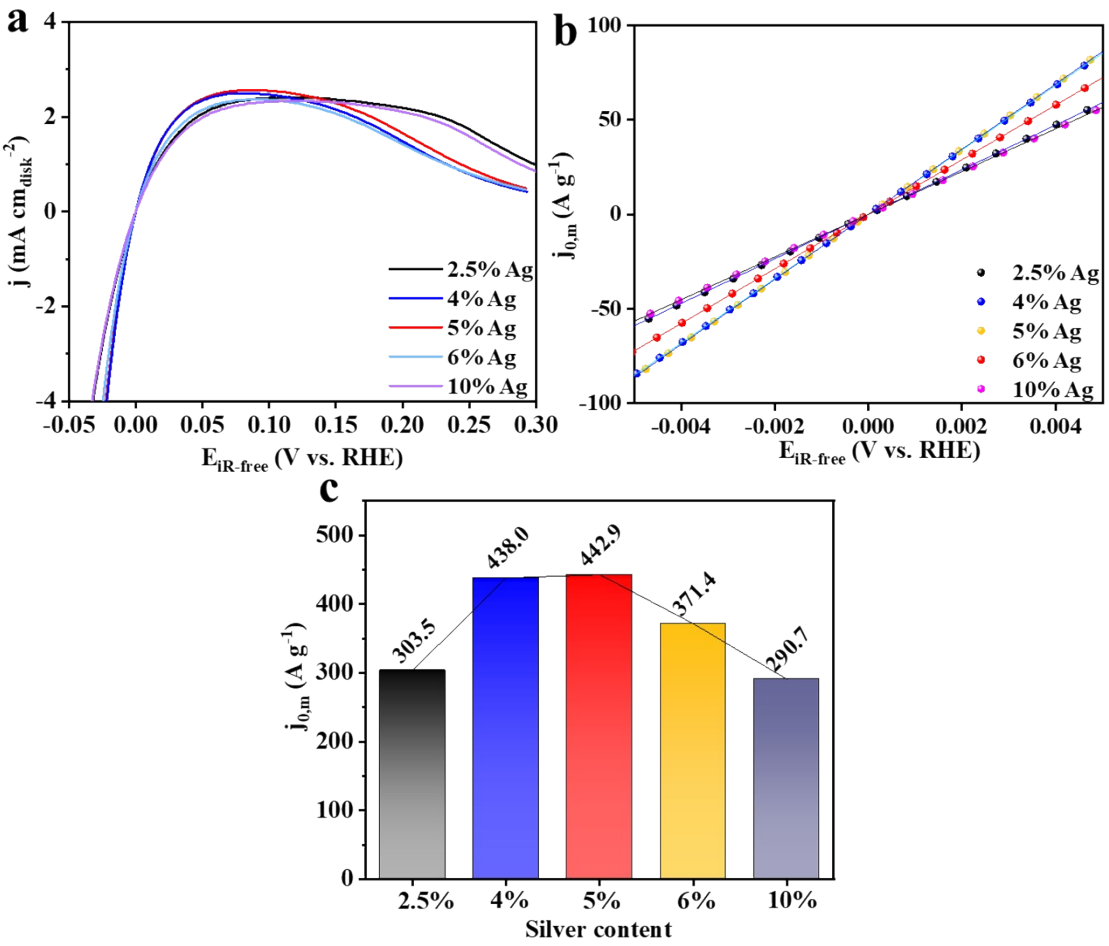

Figure S12. (a) Alkaline HOR polarization curves; (b) micro-polarization region and linearly fitted curves from -5 to 5 mV vs. RHE according to micropolarization Bulter-Volmer equation; (c) $j_{0,m}$ of RuAgW/C with different molar ratio between Ag and Ru precursors.

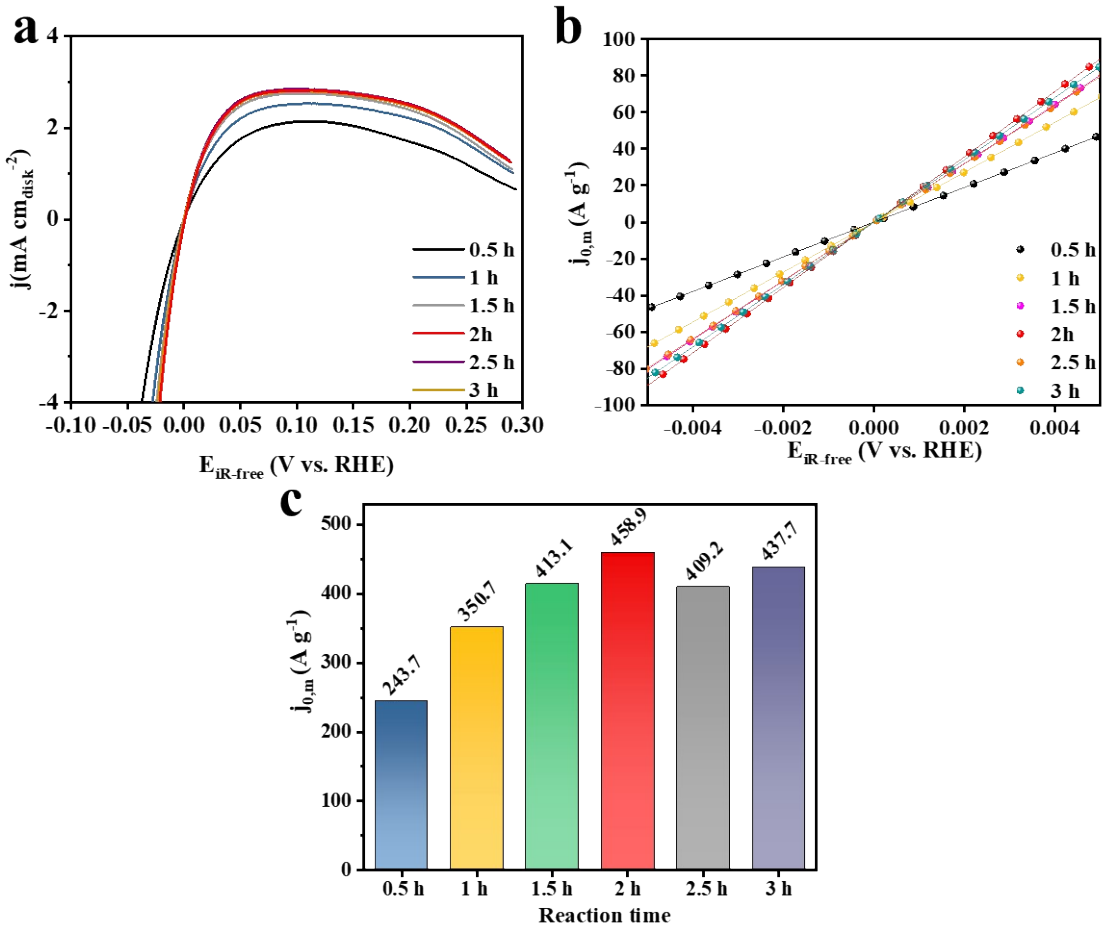

Figure S13. (a) Alkaline HOR polarization curves; (b) micro-polarization region and linearly fitted curves from -5 to 5 mV vs. RHE according to micropolarization Bulter-Volmer equation; (c) $j_{0,m}$ of RuAgW/C with different chemical reduction time.

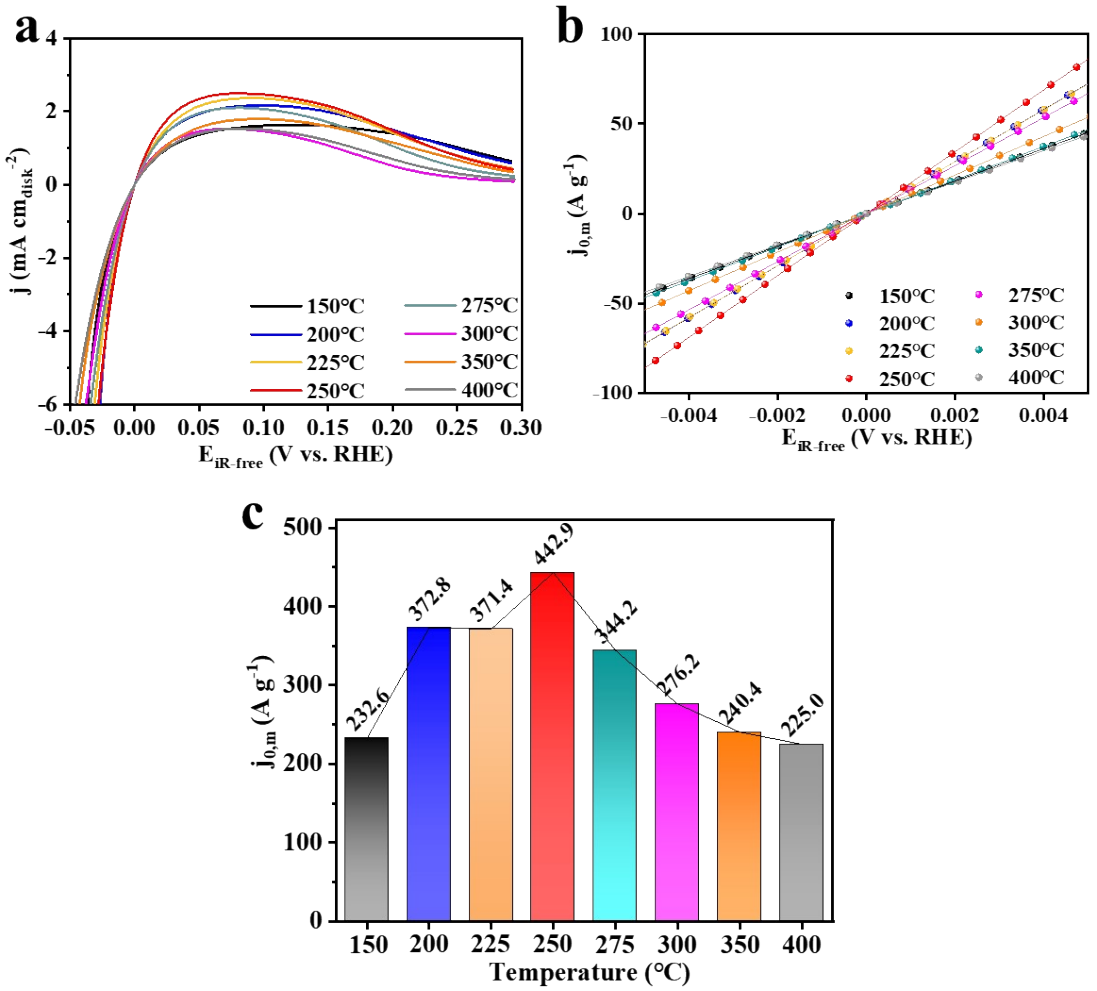

Figure S14. (a) Alkaline HOR polarization curves; (b) micro-polarization region and linearly fitted curves from -5 to 5 mV vs. RHE according to micropolarization Bulter-Volmer equation; (c) $j_{0,m}$ of RuAgW/C heat-treated at different temperatures.

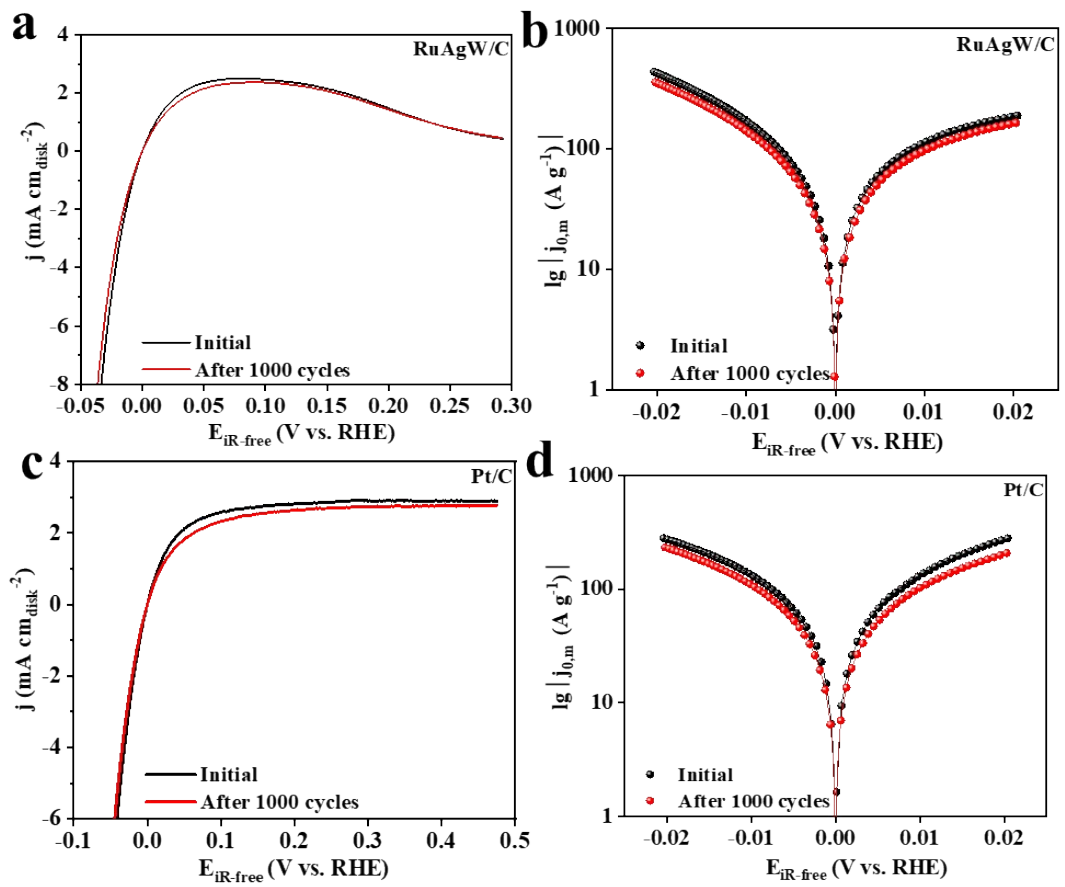

Figure S15. (a) Alkaline HOR polarization curves and (b) HOR Tafel plots of RuAgW/C before and after ADTs; (c) alkaline HOR polarization curves and (d) HOR Tafel plots of Pt/C before and after ADTs.

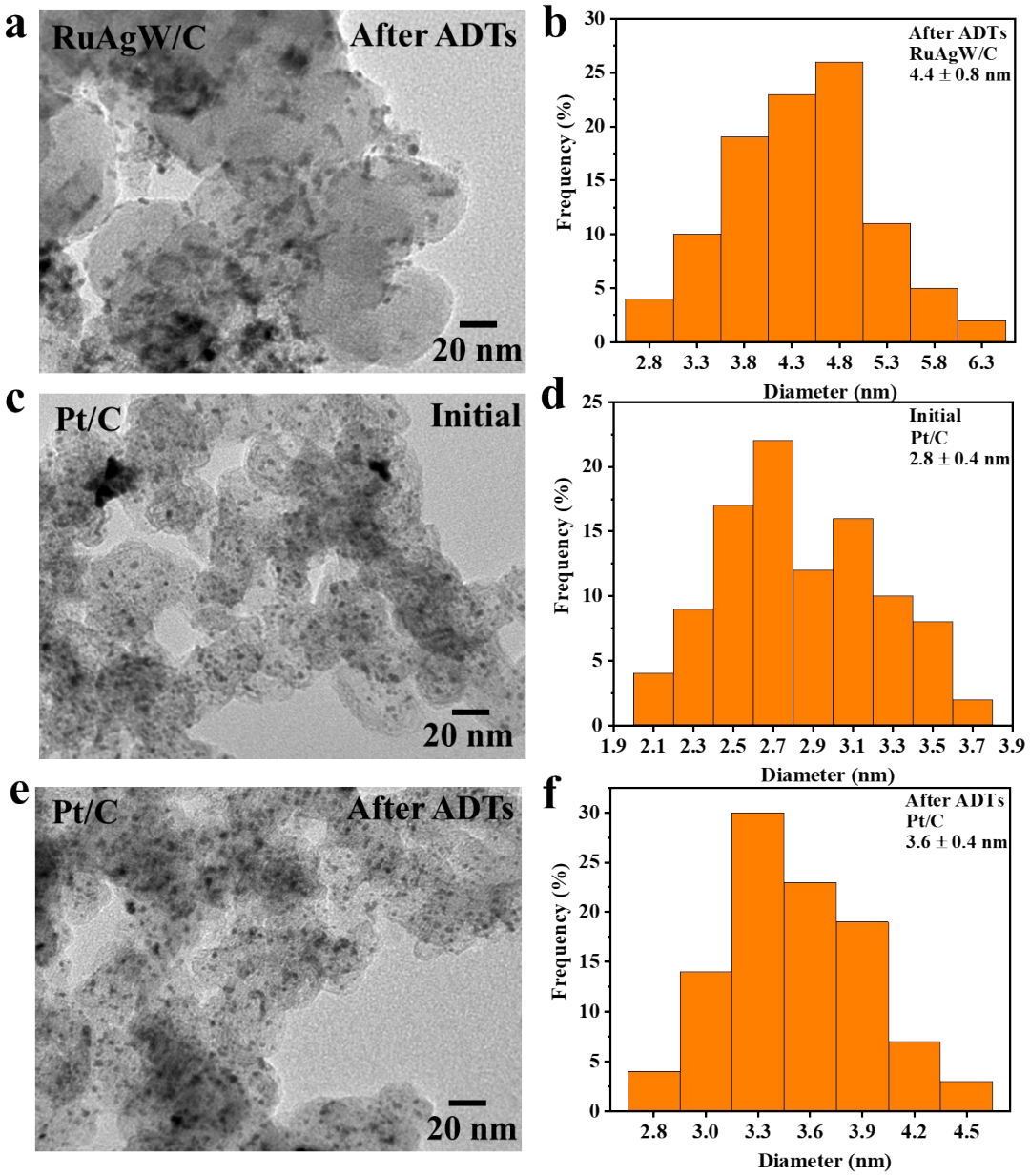

Figure S16. (a) A typical TEM image and (b) particle size distribution of RuAgW/C after ADTs; (c) a typical TEM image and (d) particle size distribution of Pt/C before ADTs; (e) a typical TEM image and (f) particle size distribution of Pt/C after ADTs.

Note: the average size and size distribution for each sample were determined by manually measuring at least 200 individual particles.

Table S1. Alkaline HOR activity of non-Pt noble metal based electrocatalysts.

Catalyst	Catalyst Loading (μg_{PGM} cm_{disk}^{-2})	Rotating Rate (rpm)	$j_{0,m}$ (A g_{PGM}^{-1})	$j_{0,s}$ (mA cm^{-2})	Reference
RuAgW/C	6.7	1600	442.9	0.77	This work
$Pd_{0.2}Ru_{0.8}$/C	7.04	2500	144	0.08	[4]
di-RuNi MLNS/C	3	1600	153	0.37	[5]
Ru-Ru_2P/C	8.33	1600	375	-	[6]
Ru-$Cr_1(OH)_x$	60	1600	96.6	0.28	[7]
fcc-Ru/C	5.0	1600	120	0.19	[8]
RuSn/C	7.45	1600	202	0.15	[9]
PdO-RuO_2/C	3.55	1600	523	0.51	[10]
Ru@NC/C-400	20.4	2500	54	0.30	[11]
Ru-TiO/TiO_2@NC	25.5	2500	42	0.27	[12]
RuNi/NC	12.6	1600	214	-	[13]
$Ru_{0.95}Co_{0.05}$/C	14	1600	290	0.11	[14]
$Ru_{2.3}Ni_1$/C	33	1600	38.8	0.04	[15]
$RuFe_{0.1}$ NS/C	3.85	1600	234	0.54	[16]
$Pb_{1.04}$-$Ru_{92}Cu_8$/C	1.8	1600	44.7	0.23	[17]
Ru_2P/C	10	1600	270	-	[18]
Ru-WC_x	1.17	1600	471	1.44	[19]
Ir_3PdRu_6/C	3.5	1600	728	0.60	[20]

Table S2. Alkaline HOR activity of RuAgW/C and home-made electrocatalysts in this work.

Catalyst	Mass specific activity （A g^{-1}）	ECSA (m^2 g^{-1})	Area specific exchange density（mA cm^{-2}）
Pt/C	329.7	80	0.41
RuAgW/C	442.9	58	0.77
RuAg/C	298.9	51	0.59
RuW/C	251.1	148	0.17
homemade Ru/C	193.5	123	0.16

References

1. S. Ghoshal, Q. Y. Jia, M. K. Bates, J. K. Li, C. C. Xu, K. Gath, J. Yang, J. Waldecker, H. Y. Che, W. T. Liang, G. N. Meng, Z. F. Ma and S. Mukerjee, *ACS Catal.*, 2017, **7**, 4936-4946.
2. X. N. Wang, Y. F. Tong, W. T. Feng, P. Y. Liu, X. J. Li, Y. P. Cui, T. H. Cai, L. M. Zhao, Q. Z. Xue, Z. F. Yan, X. Yuan and W. Xing, *Nat. Commun.*, 2023, **14**, 11.
3. Y. Z. Li, J. Abbott, Y. C. Sun, J. M. Sun, Y. C. Du, X. J. Han, G. Wu and P. Xu, *Appl. Catal. B-Environ.*, 2019, **258**, 8.
4. S. St. John, R. W. Atkinson, III, R. R. Unocic, T. A. Zawodzinski, Jr. and A. B. Papandrew, *J. Phys. Chem. C*, 2015, **119**, 13481-13487.
5. Y. T. Dong, Q. T. Sun, C. H. Zhan, J. T. Zhang, H. Yang, T. Cheng, Y. Xu, Z. W. Hu, C. W. Pao, H. B. Geng and X. Q. Huang, *Adv. Funct. Mater.*, 2023, **33**, 10.
6. L. X. Su, Y. M. Jin, D. Gong, X. Ge, W. Zhang, X. R. Fan and W. Luo, *Angew. Chem., Int. Ed.*, 2023, **62**, 8.
7. B. Zhang, B. Zhang, G. Zhao, J. Wang, D. Liu, Y. Chen, L. Xia, M. Gao, Y. Liu, W. Sun and H. Pan, *Nat. Commun.*, 2022, **13**, 5894.
8. T. H. Zhao, D. D. Xiao, Y. Chen, X. Tang, M. X. Gong, S. F. Deng, X. P. Liu, J. M. Ma, X. Zhao and D. L. Wang, *J. Energy Chem.*, 2021, **61**, 15-22.
9. L. X. Su, X. R. Fan, Y. M. Jin, H. J. Cong and W. Luo, *Small*, 2023, **19**, 9.
10. R. Samanta, R. Mishra and S. Barman, *Chem. Sus. Chem.*, 2021, **14**, 2112-2125.
11. J. Liu, B. Y. Zhang, Y. Fo, J. Gao, W. Q. Yu, H. W. Ren, X. J. Cui, X. Zhou and L. H. Jiang, *Chem. Eng. J.*, 2023, **468**, 8.
12. L. Jing, G. Jie, W. Q. Yu, H. W. Ren, X. J. Cui, X. Chen and L. H. Jiang, *Chem. Eng. J.*, 2023, **472**, 8.
13. L. L. Han, P. F. Ou, W. Liu, X. Wang, H. T. Wang, R. Zhang, C. W. Pao, X. J. Liu, W. F. Pong, J. Song, Z. B. Zhuang, M. V. Mirkin, J. Luo and H. L. L. Xin, *Sci. Adv.*, 2022, **8**, 10.
14. H. S. Wang, Y. Yang, F. J. DiSalvo and H. D. Abruña, *ACS Catal.*, 2020, **10**, 4608-4616.
15. C. P. Huang, M. C. Tsai, X. M. Wang, H. S. Cheng, Y. H. Mao, C. J. Pan, J. N. Lin, L. D. Tsai, T. S. Chan, W. N. Su and B. J. Hwang, *Catal. Sci. Technol.*, 2020, **10**, 893-903.
16. Y. Li, C. Yang, C. Ge, N. Yao, J. Yin, W. Jiang, H. Cong, G. Cheng, W. Luo and L. Zhuang, *Small*, 2022, **18**, e2202404.
17. Y. T. Dong, Z. M. Zhang, W. Yan, X. R. Hu, C. H. Zhan, Y. Xu and X. Q. Huang, *Angew. Chem., Int. Ed.*, 2023, **62**.
18. Q. Q. Yu, W. Q. Yu, Y. J. Wang, J. T. He, Y. K. Chen, H. F. Yuan, R. Y. Liu, J. J. Wang, S. Y. Liu, J. Y. Yu, H. Liu and W. J. Zhou, *Small*, 2023, **19**, 10.
19. L. Q. Wang, Z. P. Xu, C. H. Kuo, J. Peng, F. Hu, L. L. Li, H. Y. Chen, J. Z. Wang and S. J. Peng, *Angew. Chem., Int. Ed.*, 2023, **62**, 10.
20. H. S. Wang and H. D. Abruña, *J. Am. Chem. Soc.*, 2017, **139**, 6807-6810.